arXiv:1403.6634v1 [physics.plasm-ph] 26 Mar 2014

Turbulence in two dimensional visco - elastic medium

Sanat Kumar Tiwari, Vikram Singh Dharodi,
Amita Das, Bhavesh G. Patel, and Predhiman Kaw
Institute for Plasma Research, Bhat , Gandhinagar - 382428, India

(Dated: March 27, 2014)

Abstract

The properties of decaying turbulence is studied with the help of a Generalized Hydrodynamic (GHD) fluid model in the context of two dimensional visco - elastic medium such as a strongly coupled dusty plasma system. For the incompressible case considered here however, the observations are valid for a wider class of visco - elastic systems not necessarily associated with plasmas only. Our observations show that an initial spectrum that is confined in a limited domain of wave numbers becomes broad, even when the Reynold's number is much less than the critical value required for the onset of turbulence in Newtonian fluids. This is a signature of elastic turbulence where Weissenberg's number also plays a role in the onset of turbulence. This has been reported in several experiments. It is also shown that the existence of memory relaxation time parameter and the transverse shear wave inhibit the normal process (for 2-D systems) of inverse spectral cascade in this case. A detailed simulation study has been carried out for the understanding of this inhibition.

I. INTRODUCTION

The understanding of fluid flows has been of great interest in past and a significant amount of research have been dedicated to this particular area [1, 2]. The interest ranges for studies concerning laminar to turbulent flows, viscous to inviscid flows, variety of unsteady flows, fluid instabilities etc. While most of fluid flows have been found to follow Newtonian dynamics and hence standard Navier-Stokes (NS) equations applies, a range of fluid (viz. polymeric and colloidal suspensions, cellular solids) have non - Newtonian dynamics [3]. Often such fluids have characteristics which is a combination of both liquid and solid behavior. For instance in addition to having viscous nature, they also exhibit solid like elastic features. Several models have been proposed for the understanding of such non - Newtonian fluids. The combination of viscous behavior and solid like elastic features (often termed as visco - elastic fluids) in some cases have been depicted by introducing a memory relaxation time in the model description. Such a model is termed as Generalized Hydrodynamic fluid model.

The GHD model essentially describes a medium which plays a dual role of the fluid as well as also the medium having elastic traits due to its strong coupling nature. It differs in this sense with "polymeric fluids" where the extension field of the polymer additives in a fluid medium provide elastic stresses. Such polymeric fluids are often modeled by Oldroyd B kind of models [4] which differ significantly from the GHD model. It will, however, be interesting to understand the similarities and differences between the GHD model studied here as a representative of a visco - elastic behaviour exhibited by strongly coupled systems, with that of the Polymeric fluids where elasticity arises through external polymer additives.

In recent years there have been a great deal of interest in understanding the behavior of such visco - elastic system of fluids [5–9]. The study of the properties of such unique fluids is important from the perspective of their interesting transport behavior. The transport properties of any fluid system is known to significantly get influenced by the presence of the phenomena of turbulence. It is, therefore, both interesting and important to understand the phenomena of turbulence in the context of these novel systems. Experimental work on the study of turbulence have been conducted on many such visco - elastic systems, which show that the turbulent phenomena in the context of such systems are fairly distinct when compared to Newtonian hydrodynamics. For instance, experiments on Polymeric flows have shown onset of turbulence even when the Reynold's number is less than the critical value

for the onset of turbulence for normal Newtonian fluid systems [10, 11]. The power spectral behaviour is also different in this case.

As mentioned in the beginning, the visco - elastic medium is often represented by a Generalized Hydrodynamic (GHD) model with a memory relaxation time parameter to represent elasticity features in the medium. This model has been found to adequately represent various experimental observations in both linear and nonlinear regimes. For instance, the dusty plasma medium in the intermediate range of coupling parameter Γ (ratio of inter-particle potential energy to its thermal energy) has both fluid as well as solid like traits. A Generalized Hydrodynamic (GHD) description mimicking the visco -elastic nature has been employed to study this medium [12]. The model has successfully predicted the existence of transverse shear waves which was later verified in experiments [12, 13]. Numerical evidence for the existence of transverse shear waves, singular cusp structures [14–16] have also been provided. Numerical studies in 2-D have also indicated the formation and the sustained presence of short scale structure, a characteristic significantly different than that of the 2-D hydrodynamic flows, which exhibits inverse cascade in two dimension.

Keeping this in view, the prime objective of the manuscript is to study the phenomena of turbulence in visco - elastic medium by numerically simulating the GHD model description. A detailed study of the spectral cascade behavior in 2-D for such systems has been carried out. We restrict our studies here to the simplified incompressible limit. This helps us in investigating the role of pure transverse shear waves (an attribute of elasticity in the medium) in such studies. The extraneous effects due to compressible fluctuations have been ignored at the moment. As the incompressible limit of GHD model assumes no density perturbations, in the context of strongly coupled dusty plasma medium this corresponds to the absence of any charge fluctuations. The results obtained here, represent a wide range of fluid flows and not merely the strongly coupled plasma system, which would be represented with such a visco-elastic prescription.

The paper has been organized as follows. A brief description of the governing equations for such an incompressible GHD model and the numerical procedure adopted for the simulation studies have been provided in section II. Section III contains the results of our numerical simulation. The theoretical analysis and discussion has been provided in section IV. Section V contains the conclusion.

II. GOVERNING EQUATIONS

The behavior of visco - elastic fluids can be represented by a Generalized Hydrodynamic description. In this description, the normalized momentum equation is expressed as [16, 17]:

$$\left[1+\tau_m\left(\frac{\partial}{\partial t}+\vec{v}\cdot\nabla\right)\right]\left[\left(\frac{\partial}{\partial t}+\vec{v}\cdot\nabla\right)\vec{v}+\frac{\nabla P}{n}\right]=\eta\nabla^2\vec{v} \tag{1}$$

In the absence of compressible fluctuations, the equation of state takes the form of

$$\nabla\cdot\vec{v}=0 \tag{2}$$

Here, $\vec{v}, n$ and P are the velocity, density and pressure fields of the visco - elastic fluid respectively. The parameter τ_m, is known as the time relaxation parameter and is associated with the typical time duration for which the visco - elastic medium retains the memory of past configurations. Here, η is the kinematic viscosity, whose finite value causes viscous dissipation and is also responsible for elastic wave propagation in the medium, depending on whether one is observing phenomena with time scales longer or shorter than the relaxation time parameter respectively. For a strongly coupled medium the parameters η and τ_m are dependent on each other. The empirical relationship between the two have been written down for several strongly coupled fluid systems [12, 18]. For the case of strongly coupled plasmas, the value of these two parameters depends on the coupling parameter Γ which is the ratio of inter particle potential energy to the average thermal energy of the species [12]. The normalization used for the above Eqs. (1,2) is as follows. The length and time are normalized with L_0 and T_0, which are respectively the typical length and time scale of the system under consideration. The density is normalized with a typical density of system N_0. These normalizations are conveniently chosen so that one has to primarily deal with numbers of the order of unity in simulation and analysis for any system. The relaxation parameter τ_m is also normalized with T_0. The normalized kinematic viscosity $\eta_N = \eta/mnU_0L_0$ and the normalized pressure $P_N = P/mnU_0^2$, where $U_0 = L_0/T_0$. We can also see from here that the normalized viscosity $\eta_N = 1/R_e$, is essentially the inverse of Reynold's number. The Reynold's number being a dimensionless number defined as the ratio of nonlinearity to dissipation, characterizes the typical flow of any fluid system. Another important dimensionless number associated with viscoelastic flows is the Weissenberg number $W_i = U_0\tau_m/L_0 = \tau_{mN}$. The Weissenberg number is essentially the ratio of the memory relaxation time to the typical eddy turn over

time of the system. It thus characterizes the elastic behavior of the medium. Some recent experiments have shown that the elastic turbulence can be excited even in the regime of low R_e provided the Weissenberg number W_i is high [10, 11]. We have chosen similar regime of parameter space for our present studies and observe that the spectrum becomes broad asymptotically even if it is initially confined in a limited domain. In Fig. 1, we have made an attempt to locate the values of typical R_e and W_i for which turbulence has been observed in the context of a variety of fluid flow systems. We can easily visualize that if we go along the x-axis, we follow the hydrodynamic flows, these flows for $R_e > 10^5$ show turbulent features. The lowest possible value of R_e over this axis for which the turbulent flows have been reported is $R_e \approx 2500$ by Avila et. al [19]. In the $W_i - R_e$ plane, we have indicated points where elastic turbulence studies have been conducted. In the figure symbols with red filled box show the points where turbulence has been observed in experiments by Groismann et al. [10] and those experiments conducted by Burghela et al. [20] square shaded region respectively. Simulations for visco-elastic fluids have also been performed using different models and their corresponding positions have been shown by black dots (Berti et al. using Oldroyd-B model) and those represented by blue circle, box and star symbols are by Sanat et al. using Generalized Hydrodynamic model [4, 16, 21]. It is clear from the figure that elastic turbulence occurs for those values of Reynolds number which are much smaller than the critical value of Reynolds number necessary for turbulence in pure hydrodynamic systems.

For the purpose of numerical simulation we reduce the second order Eq. (1) in time to two coupled first order equations satisfying the following convective forms.

$$\left[1 + \tau_m \left(\frac{\partial}{\partial t} + \vec{v} \cdot \nabla\right)\right] \vec{\Psi} = \eta \nabla^2 \vec{v} \tag{3}$$

$$\left[\left(\frac{\partial}{\partial t} + \vec{v} \cdot \nabla\right) \vec{v} + \frac{\nabla p}{n}\right] = \vec{\Psi} \tag{4}$$

In the 2-D incompressible case, with the flow confined in the 2-D plane normal to the symmetry axis we can represent the velocity field by a scalar potential Φ, satisfying $\hat{z} \times \nabla\Phi = \vec{v}$. Here $\hat{z}$ is directed along the symmetry axis. Taking the curl of Eq. (4) we have

$$\left[\frac{\partial}{\partial t} + \hat{z} \times \nabla\Phi \cdot \nabla\right] \nabla^2\Phi = (\nabla \times \Psi)_z = \left(\frac{\partial \Psi_y}{\partial x} - \frac{\partial \Psi_x}{\partial y}\right) \tag{5}$$

We can construct the following evolution equations for the square integral quantities by

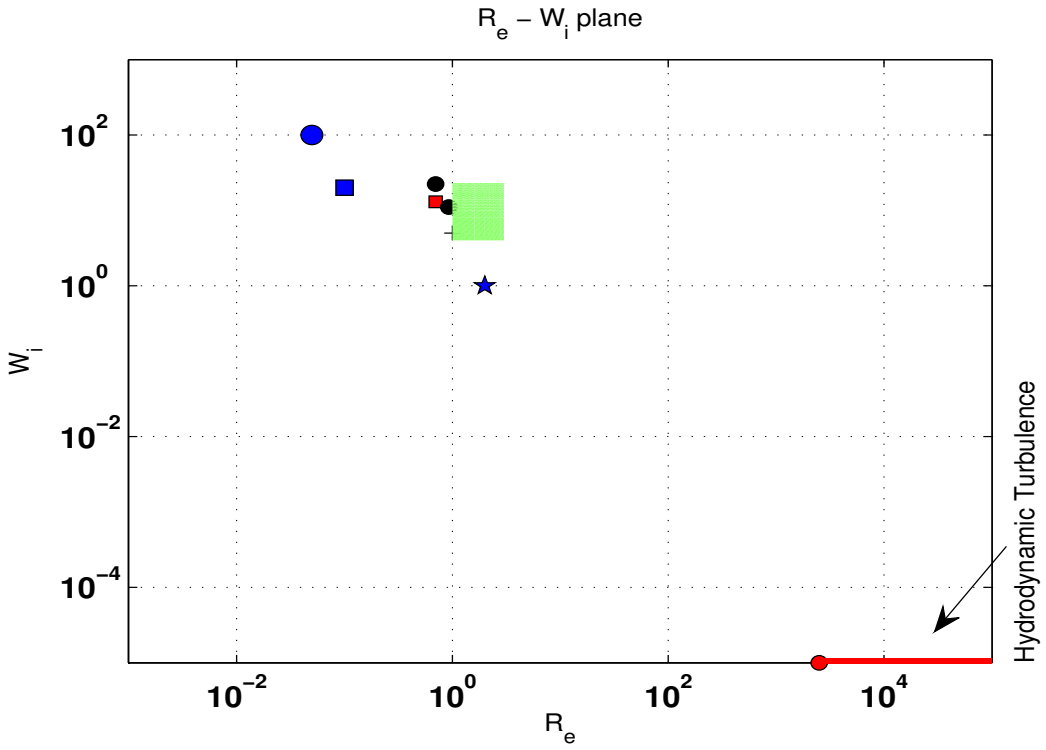

FIG. 1: Red line with circle (—○) shows the regime of Hydrodynamic turbulence with its starting point at $R_e \approx 2500$ [19]. Black dots (•) show the regime of elastic turbulence simulation by Berti et. al. using Oldroyd-B model [4]. Blue circle, square and pentagon (○, □, ★) are the points on $R_e - W_i$ plot where authors have contributed ; the work has been presented here as well as in some previous publications [16, 21]. Plus (+) is point where Molecular dynamics simulations have been performed for strongly coupled Yukawa fluids [22]. Red square (□ point outs regime where some recent experiments have been performed by Groisman et. al [10]). The shaded square region covers area in which studies made by Burghelea et. al [20].

taking the scalar product of $\vec{v}$ with Eq. (4) and $\vec{\Psi}$ with Eq. (3) respectively

$$\frac{1}{2}\frac{\partial}{\partial t}\int\int v^2 dxdy = \int\int \vec{v}\cdot\vec{\Psi} dxdy \tag{6}$$

$$\frac{1}{2}\frac{\partial}{\partial t}\int\int \Psi^2 dxdy = -\frac{1}{\tau_m}\int\int \Psi^2 dxdy + \frac{\eta}{\tau_m}\int\int \vec{\Psi}\cdot\nabla^2\vec{v} dxdy \tag{7}$$

The evolution of these quantities are tracked during the course of numerical simulation for the purpose of determining the accuracy of the simulation.

A random spectrum of initial fluctuations is prescribed, whose evolution is tracked with the help of numerical simulation. For this purpose we employ the following two choices of

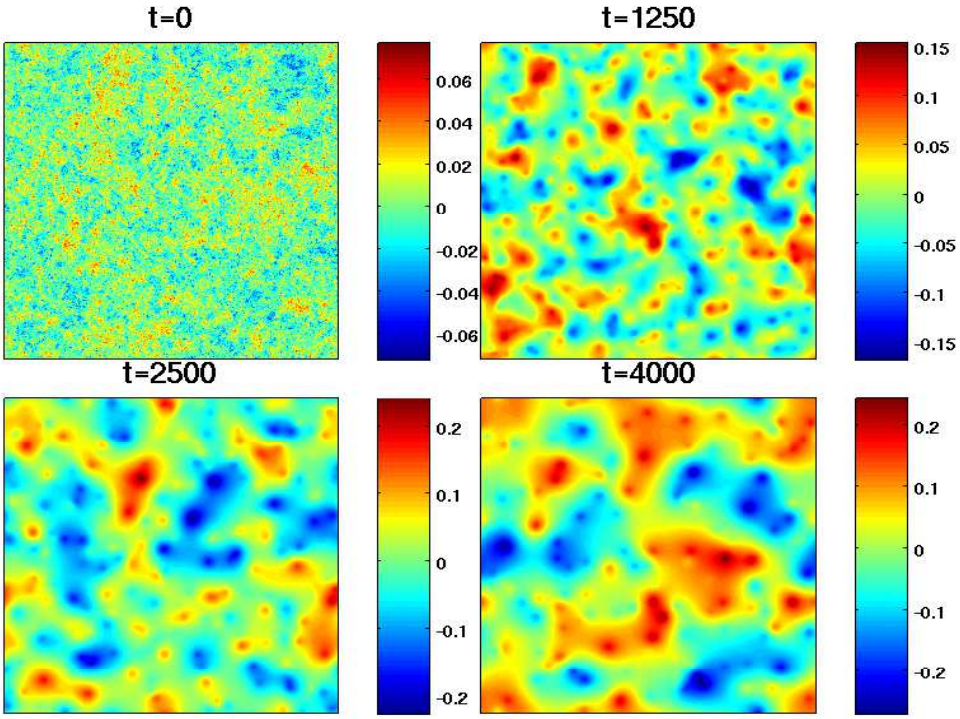

FIG. 2: Evolution of a random initial configuration of velocity potential Φ with the GH code reproducing the incompressible hydrodynamic fluid limit for very small values of τ_m and η. The inverse spectral cascade is clearly evident from the formation of long scale structures.

initial distribution of power in the velocity potential field Φ for our studies:

$$\mid \Phi_k \mid^2 = \frac{C}{(1+ \mid k \mid)^n} \tag{8}$$

$$\mid \Phi_k \mid^2 = C sech^2 \left(\frac{\mid k \mid - k_m}{4} \right) \tag{9}$$

Here, C is constant which decides the level of power injected in system. The individual Fourier modes in the spectrum are chosen to have random phases with spectral weights provided by either by Eq. (8) or Eq. (9). In the first choice, the power falls of monotonically with wave number (the rapidity of fall being governed by the index n) and in the latter choice the peak of the initial spectrum can be chosen at any desired wavenumber determined by the value of k_m. Furthermore, in the simulations presented here, we have restricted to an initial choice of $\vec{\Psi} = 0$. These two different choices of the initial spectrum help us in ascertaining the dependence if any on initial conditions on evolution. This is important in the context of GHD where the medium is expected to retain memory for some time. These

initial conditions are then evolved using the Eqs. (3,5) through a flux corrected scheme [23]. In the next section we present the details of some interesting observations obtained from our simulation studies.

We also note that the general dispersion relation for transverse shear waves obtained from Eq. (1) is

$$\omega = \frac{-i}{2\tau_m} \pm 0.5\sqrt{\frac{-1}{\tau_m^2} + \frac{4\eta k^2}{\tau_m}} \tag{10}$$

This dispersion relation suggests that the transverse waves can propagate in the visco-elastic medium only for those wavenumbers which satisfy the criteria of $k > \sqrt{1/4\eta\tau_m}$. For most of the simulations performed in this paper, we have taken $\eta = 5$ and $\tau_m = 20$ which gives a critical wavevector $k = k_c = 2.5 \times 10^{-3}$. In our simulations, we have taken $L_x = L_y = 20$ (system length in X and Y direction respectively), and $Nx = Ny = 1024$ (or 500 in some cases). Where Nx and N_y are the grid points in X and Y direction respectively. The longest mode corresponding to this system will be $k_0 = 0.3142 > k_c$. Thus, in our system, the permissible wave numbers are such that the transverse shear mode corresponding to them have propagating characteristic.

III. NUMERICAL OBSERVATIONS

We use the numerical procedure outlined in Section II to reproduce the known case of the hydrodynamic (HD) fluid system. For this purpose we have carried out simulations for $\eta = 0$ and chosen τ_m to be very small. In Fig. 2 the velocity potential contours for this case has been shown at various times. The initial spectrum was chosen to be provided by Eq. (8) with n = 2. The formation of longer scales at later times are an evidence of inverse spectral cascade as expected for the 2-D hydrodynamic case. A broad power spectra with indices of -5/3 and -3 in inverse and forward cascade regime has also been recovered for these runs for $R_e >> R_e^{crit}$.

In Fig. 3, we then show the constant contour plots of the velocity potential Φ for the visco - elastic case having $\eta = 5, \tau_m = 20$. In this case too, the initial form of velocity potential is given by Eq. (8) with $n = 2$. It is clear from the figures that the evolution for the visco -elastic case is very different. For the HD case one observes a progressive formation of longer scales which ultimately yielded few isolated vortex structures of the order of system size. On the

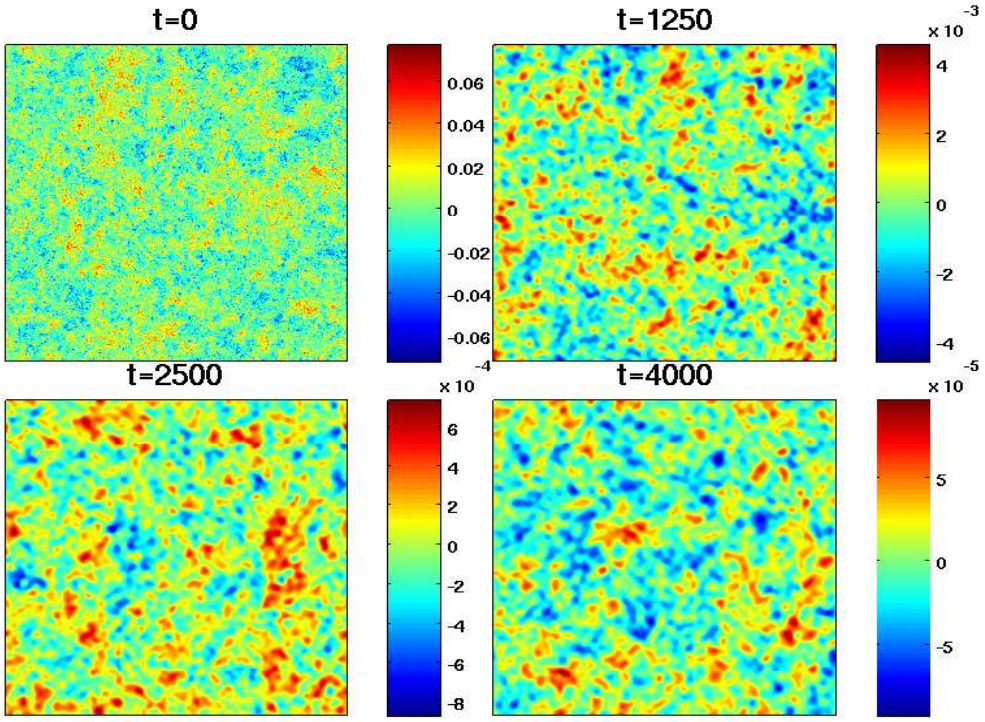

FIG. 3: Evolution of phase randomized velocity potential for incompressible visco-elastic fluids. It could be seen that in contrast to hydrodynamic fluids, much shorter structures are present in this particular case. The parameters η and τ_m are 5 and 20 respectively.

other hand, for visco - elastic case shown in Fig. 3 the time asymptotic state shows a clutter of closely packed structures which typically continue to be sustained even though their size is much smaller than that of the simulation box dimension. To have a quantitative assessment we have also monitored the evolution of mean square averaged wavenumber $< k^2 >$ for the two cases, which has been shown in Fig. 4. It is clear from the figure that in both HD and the visco - elastic case described by GHD cases the spectral cascade is towards longer scales as the value of $< k^2 >$ is found to decrease. However, for the case of visco -elastic system in GHD (now onwards referred as GHD case) this happens much slowly. Furthermore, the asymptotic value of the mean square averaged wave number is higher (implying sustainment of shorter scales) in GHD as compared to the HD case. Thus, even GHD system seems to exhibit the 2-D inverse cascade behavior to some extent albeit a bit slowly. It is well known though that in the context of 2-D NS dynamics representing HD flows that the phenomena of inverse spectral cascade is related to the preservation of two integral square invariants for by the equations. The GHD equations,however, do not support two integral square invariants.

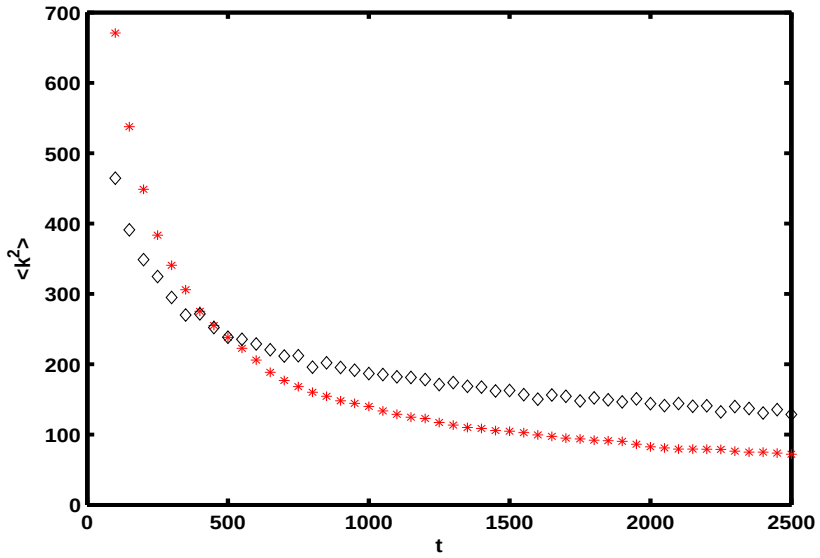

FIG. 4: The plot of $< k >^2$ with time for the GHD case with ($\eta = 5$ and $\tau_m = 20$) (square) and for the incompressible fluid (circle). the initial random flow has been taken of the form given by Eq. (8) with $n = 2$.

These simulations being that of undriven and dissipative nature (e.g. in both HD and GHD cases η is responsible for viscous damping, in GHD it also has an additional role of elasticity in the medium), the overall power spectrum decreases with time. However, we observe that with time the spectrum attains an asymptotic form which has been shown in Fig. 5. This GHD spectrum is in stark contrast to the HD case. The observed spectrum is broad, even though the Reynold's number ($R_e = \eta^{-1} = 0.2$) corresponding to these simulations is lower than R_e^{crit}. Here, the Weisenberg number $Wi = 20$. This is a feature of characteristic elastic turbulence and has been reported in experimental observations also [11]. The observed broad spectrum, however, does not have any specific power law dependence. The spectrum, instead is overwhelmed by the appearance of peaks at certain wave numbers. This indicates that the cascade process is severely inhibited at certain wave numbers, resulting in the piling up of the spectral power near certain wavenumbers location. The peaks are not sharp though and their location and shape is found to depend on the initial choice of the spectrum. This is evident from a detailed study carried out with different choices of the initial spectrum, e.g. using the two forms shown in Eqs. (8) and (9) with different values

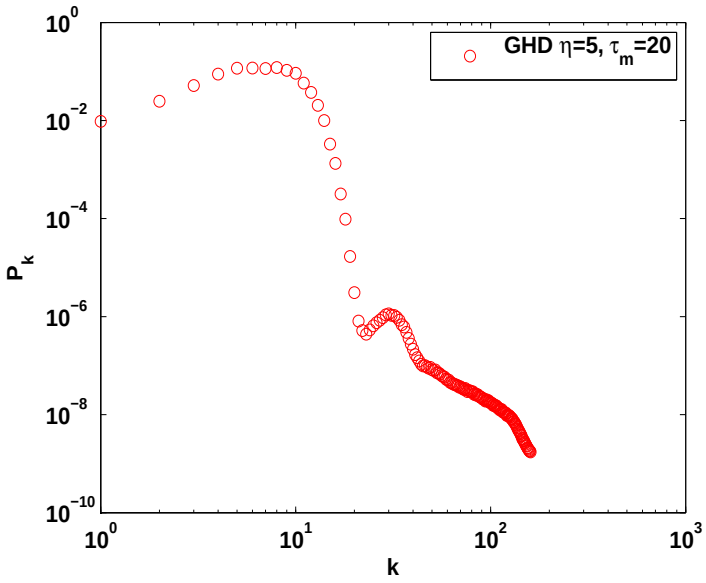

FIG. 5: Power spectra for incompressible visco-elastic fluids ($\eta = 5$ and $\tau_m = 20$).

of parameters n and k_m chosen for the study. It is clear from the Figs. 6 and 7 that for each and every GHD case, there is a perceptible shift of the location of the peak towards longer scales with time. It is also clear from the plots that the evolved spectra depends on the initial choice of spectral power distribution. We observe that the peak representing the accumulation of power gets prominent as the initial deployed power at shorter scales is increased. For instance, one can observe that when either the value of n in Eq. (8) is decreased or that of k_m increased for Eq. (9) (representing the two choices of initial form of the spectrum) the evolved spectra shows increasing dominance of the peak. We also observe that the location of the peak depends on the choice of the parameter η/τ_m. In Fig. 8 we plot the power spectra for several cases with different values of the parameter η/τ_m. It can be seen that there is a definite shift of the spectra towards high k values as the value of η/τ_m is reduced.

To summarize, the main observations of our simulations are (i) a broad non universal character of the evolved spectrum for GHD, which shows strong dependence on the initial spectrum (ii) appearance of broad peaks which shift towards longer scales with increasing time (iii) with increasing η/τ_m the peak location again shifts towards long scales (iv) The peaks are dominant when the initial power content in shorter scales is high. In the next section we provide a discussion on these observations.

IV. DISCUSSION

A hydrodynamic fluid in the incompressible limit is a scale free system as it does not support any normal mode and neither does it have any intrinsic length and/or time scale associated with it. This results in a power law spectrum at intervening scales where neither forcing nor dissipation is directly effective. In contrast, the incompressible GHD model supports transverse shear wave mode and there also exists a special time scale defined by the relaxation parameter τ_m in the system. The presence of these special scales in the GHD model is responsible for introducing features different from the power law behavior in the spectrum.

Furthermore, the HD system in 2-D supports two square integral invariants in the non dissipative limit, namely energy and enstrophy, which leads to the characteristic inverse cascade phenomena in the context of 2-D HD system. It is noteworthy here that the 3-D HD system does not support the enstrophy invariant and the spectral cascade is direct in this case. The GHD system also does not support the enstrophy invariant and hence one would have expected only a direct spectral cascade in this case.

In the case of GHD, however, we still observe formation of longer scales though it is at a considerable slower time scale here. Furthermore, the structures that form are much shorter than the box size (the observation of peaks in the spectrum testifies to it). The accumulation at intervening scales is higher when the initial spectrum has comparatively higher power in short scales. Also, one observes the shifting of peaks towards longer scales with time. This suggests that even though the GHD system does not support the second enstrophy invariant, there is a slow (compared to HD), but perceptible transfer of power towards longer scales. We now try to provide a qualitative understanding of this phenomena.

It should be noted that there is an inherent slow dynamics of HD involved in the GHD system of equations, occurring at time scales longer than the memory relaxation time τ_m. This is apparent from Eq. (1), when the $\tau_m d/dt$ can be ignored in comparison to unity. In this limit the GHD equations reduce to the HD form. This suggests that phenomena with typical times scales longer than the memory relaxation time and/or any other time associated with the elastic nature of the fluid the GHD system may contribute towards inverse spectral cascade. This is indeed what one observes in the simulation. There appears, thus, a competition between the HD dynamics of inverse spectral cascade which is opposed by the

intrinsic elastic behaviour of the system. This competition would be characterized in terms of the time scale exceeding those associated with the visco - elastic GHD interactions. The GHD is characterized by the relaxation parameter τ_m. The GHD dynamics also involves the propagation of transverse shear wave with the phase velocity $V_p = \sqrt{\eta/\tau_m}$. The time scale intrinsic to the system associated with the transverse shear wave at any given wavenumber k_s would then be $t_{sk} \sim 1/k_s V_p$. Thus at a given time t the hydrodynamic response will start playing a role in the GHD system only when the condition $t/t_{sk} >> 1$ gets satisfied. An approximate qualitative understanding of the observations can be developed along the following lines. For a particular system with predefined η and τ_m, V_p is constant. Thus at higher wavenumbers $t/t_{sk} >> 1$ has a greater chance to be satisfied. The HD response of perceptible cascade towards longer scales would, therefore, occur from short scale onwards. At increasingly longer scales (lower wavenumbers) the value of t_{sk} increases making the onset of HD dynamics difficult. Thus the procedure of inverse spectral cascade is rendered more and more difficult at longer scales. The presence of inverse cascade at short scales and its absence at longer scales would result in accumulation of power at some scale length. However, with increasing time the HD response will slowly keep taking over. This results in the continuous slow process of the shifting of the peak (showing power accumulation) towards longer scales where the power is observed to accumulate.

This also explains that as one increases $\sqrt{\eta/\tau_m}$ the hydrodynamic response would set in at decreasing k values. Thus, as one increases the value of $\sqrt{\eta/\tau_m}$ the location of the peak shifts towards longer scales as can be seen from Fig. 8.

V. CONCLUSION

It has been shown that for a visco-elastic medium depicted by the GHD model, turbulence can set in even at low Reynold's number, provided the Weisenberg number is high. This is in conformity with experimental observations and other models of elastic turbulence studies (e.g. those corresponding to polymeric fluids etc.,).

It is noteworthy that the visco - elastic system considered here supports the transverse shear wave as a normal mode. The question of whether or not the natural modes and scales of the system have a role on turbulence has continued to remain an outstanding problem. Attempts have so far been made on the basis of identifying the differences predicted

theoretically on the power spectral index of a stationary turbulence state. This has so far proved an extremely difficult exercise and has resulted in endless controversies without settling the issue one way or the other.

Against this backdrop we have shown that for the case of turbulence in visco - elastic medium governed by the Generalized Hydrodynamic equation, the quasi - stationary behavior of the turbulent spectrum provides ample evidence of the involvement of the memory relaxation time τ_m and the transverse shear wave in the spectral cascade process.

Furthermore, the appearance of shorter scales in 2-D for GHD system is also suggestive of enhanced transport and mixing properties of the GHD system vis. a vis that of 2-D HD dynamics.

---

[1] G. K. Batchelor. *An Introduction to Fluid Dynamics*. Cambridge University Press, 2000.

[2] L. G. Leal P. H. Steen M. Samimy, K. S. Breuer. *A Gallery of Fluid Motion*. Cambridge University Press, 2003.

[3] R. B. Bird, R. C. Armstrong, and O. Hassager. *Dynamics of Polymeric Liquids*. Wiley-Interscience Publication, 1987.

[4] S. Berti and G. Boffetta. Elastic waves and transition to elastic turbulence in a two-dimensional viscoelastic kolmogorov flow. *Phys. Rev. E*, 82:036314, Sep 2010.

[5] Anne Le Goff, Pablo Cobelli, and Guillaume Lagubeau. Supershear rayleigh waves at a soft interface. *Phys. Rev. Lett.*, 110:236101, Jun 2013.

[6] L. Pan, A. Morozov, C. Wagner, and P. E. Arratia. Nonlinear elastic instability in channel flows at low reynolds numbers. *Phys. Rev. Lett.*, 110:174502, Apr 2013.

[7] M. Brust, C. Schaefer, R. Doerr, L. Pan, M. Garcia, P. E. Arratia, and C. Wagner. Rheology of human blood plasma: Viscoelastic versus newtonian behavior. *Phys. Rev. Lett.*, 110:078305, Feb 2013.

[8] Piotr Habdas, Eric R. Weeks, and David G. Lynn. Squishy materials. *The Physics Teacher*, 44(5):276–279, 2006.

[9] R. S. Lakes. Viscoelastic measurement techniques. *Review of Scientific Instruments*, 75(4):797–810, 2004.

[10] A. Groisman and V. Steinberg. Elastic turbulence in a polymer solution flow. *Nature*, 405:53–

55, 2000.

[11] Alexander Groisman and Victor Steinberg. Elastic turbulence in curvilinear flows of polymer solutions. *New Journal of Physics*, 6(1):29, 2004.

[12] P. K. Kaw and A. Sen. Low frequency modes in strongly coupled dusty plasmas. *Phys. Plasmas*, **5**(10):3552–3559, 1998.

[13] J. Pramanik, G. Prasad, A. Sen, and P. K. Kaw. Experimental observations of transverse shear waves in strongly coupled dusty plasmas. *Phys. Rev. Lett.*, 88(17):175001, Apr 2002.

[14] Sanat Kumar Tiwari, Amita Das, Predhiman Kaw, and Abhijit Sen. Observation of sharply peaked solitons in dusty plasma simulations. *New Juornal of Physics*, 14:063008, 2012.

[15] Sanat Kumar Tiwari, Amita Das, Predhiman Kaw, and Abhijit Sen. Longitudinal singular response of dusty plasma medium in weak and strong coupling limits. *Physics of Plasmas*, 19(1):013706, 2012.

[16] Sanat Kumar Tiwari, Amita Das, Dilip Angom, Bhavesh G. Patel, and Predhiman Kaw. Kelvin-helmholtz instability in a strongly coupled dusty plasma medium. *Physics of Plasmas*, 19(7):073703, 2012.

[17] J.Frenkel. *Kinetic Theory Of Liquids*. Dover Publications, 1955.

[18] Setsuo Ichimaru. Strongly coupled plasmas: high-density classical plasmas and degenerate electron liquids. *Rev. Mod. Phys.*, 54:1017–1059, Oct 1982.

[19] Kerstin Avila, David Moxey, Alberto de Lozar, Marc Avila, Dwight Barkley, and Björn Hof. The onset of turbulence in pipe flow. *Science (New York, N.Y.)*, 333(6039):192–6, July 2011.

[20] Teodor Burghelea, Enrico Segre, and Victor Steinberg. Elastic turbulence in von karman swirling flow between two disks. *Physics of Fluids (1994-present)*, 19(5):–, 2007.

[21] Sanat Kumar Tiwari, Amita Das, Bhavesh G. Patel, and Predhiman Kaw. Kelvin-helmholtz instability in visco-elastic fluids. *Submitted to AIP proceedings*.

[22] J Ashwin and R Ganesh. Kelvin Helmholtz Instability in Strongly Coupled Yukawa Liquids. *Physical Review Letters*, 215003(May):1–4, 2010.

[23] J.P. Boris, A.M. Landsberg, E.S. Oran, and J.H. Gardner. Lcpfct - a flux-corrected transport algorithm for solving generalized continuity equations. Technical Report NRL Memorandum Report 93-7192., Navel Research Laboratory, 1993.

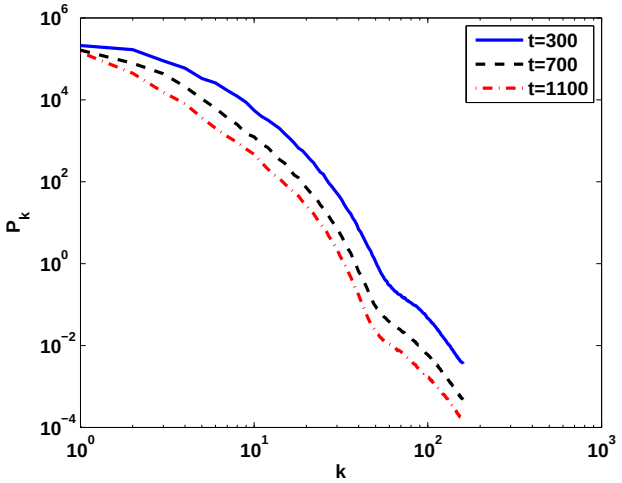

(a) $\mid \phi_k \mid^2 = Csech^2(\frac{|k|-20}{4})$

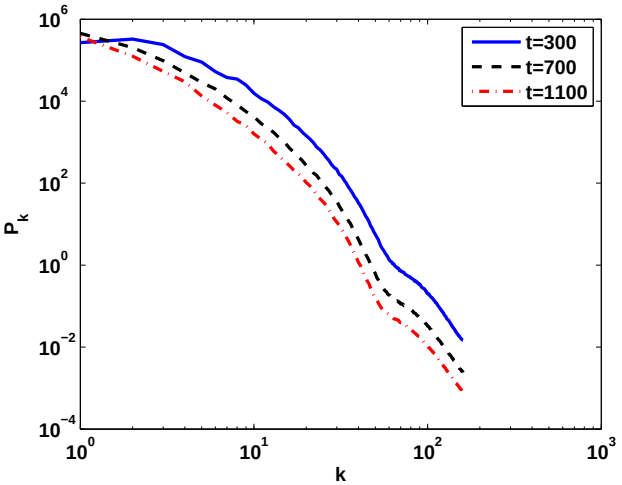

(b) $\mid \phi_k \mid^2 = Csech^2(\frac{|k|-30}{4})$

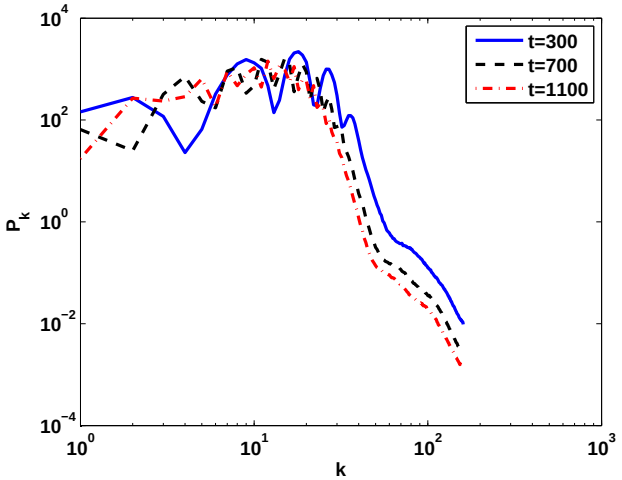

(c) $\mid \phi_k \mid^2 = Csech^2(\frac{|k|-90}{4})$

FIG. 6: Power spectra for incompressible visco-elastic fluids with different initial form of spectrum mentioned alongside. For the subplots (a), (b) and (c), the initial power has been injected at $k_m = 20, 30$ and $k_m = 90$ respectively.

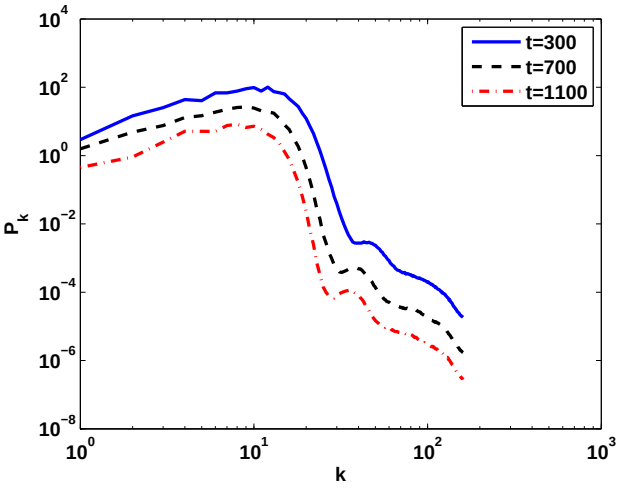

(a) $\mid \phi_k \mid^2 = \frac{C}{(1+|k|)^8}$

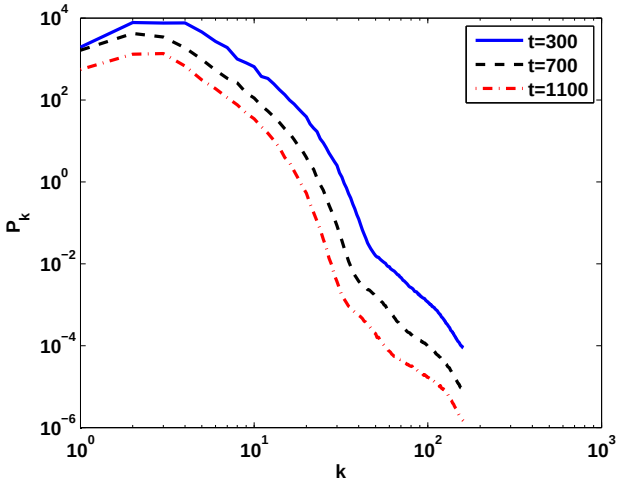

(b) $\mid \phi_k \mid^2 = \frac{C}{(1+|k|)^4}$

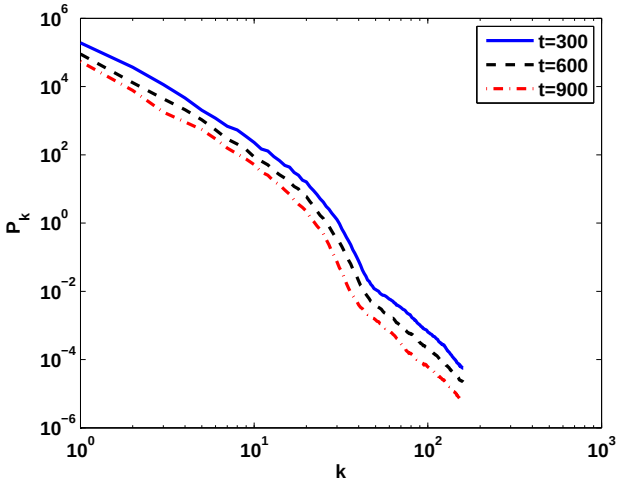

(c) $\mid \phi_k \mid^2 = \frac{C}{(1+|k|)^2}$

FIG. 7: Power spectra with different initial form of spectrum (monotonically distributed power) mentioned alongside. For the subplots (a), (b) and (c), the initial power has been injected as given in Eq. (8) with $n = 8, 4$ and $n = 2$ respectively.

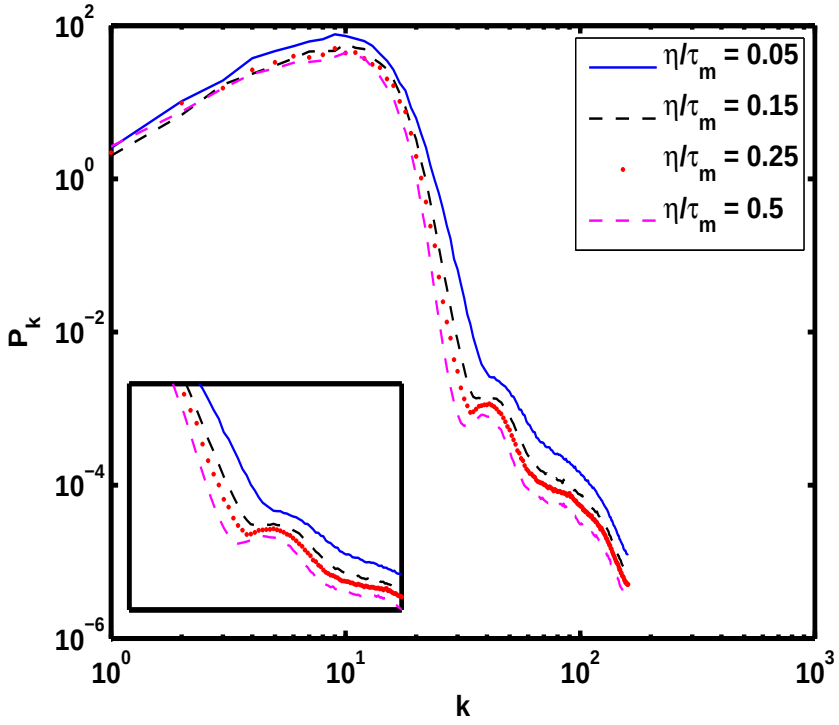

FIG. 8: Power spectra plots with different value of η/τ_m for incompressible visco-elastic fluid. The initial form of velocity potential is given as in Eq. (8) with $n = 2$. The spectra for all values of η/τ_m has been plotted here at $t = 500$.